

1 HLA-A*01:01 allele vanishing in COVID-19 2 patients population associated with non- 3 structural epitope abundance in CD8+ T- 4 cell repertoire

5
6 Maxim Shkurnikov^{1*}, Stepan Nersisyan^{1,2,3,4}, Darya Averinskaya¹, Milena Chekova¹, Fedor
7 Polyakov¹, Aleksei Titov⁵, Dmitriy Doroshenko⁶, Valery Vechorko⁶, Alexander Tonevitsky^{1,2*}

8
9 ¹Faculty of Biology and Biotechnology, HSE University, Moscow, Russia

10 ²Shemyakin-Ovchinnikov Institute of Bioorganic Chemistry, Russian Academy of Sciences,
11 Moscow, Russia

12 ³Institute of Molecular Biology, The National Academy of Sciences of the Republic of Armenia,
13 Yerevan, Armenia

14 ⁴Armenian Bioinformatics Institute (ABI), Yerevan, Armenia

15 ⁵National Research Center for Hematology, Moscow, Russia

16 ⁶O.M. Filatov City Clinical Hospital, Moscow, Russia

17

18 *Correspondence: mshkurnikov@hse.ru, atonevitsky@hse.ru

19

20

21 Abstract

22

23 In mid-2021, the SARS-CoV-2 Delta variant caused the third wave of the COVID-19 pandemic
24 in several countries worldwide. The pivotal studies were aimed at studying changes in the
25 efficiency of neutralizing antibodies to the spike protein. However, much less attention was
26 paid to the T-cell response and the presentation of virus peptides by MHC-I molecules. In this
27 study, we compared the features of the HLA-I genotype in symptomatic patients with COVID-
28 19 in the first and third waves of the pandemic. As a result, we could identify the vanishing of
29 carriers of the HLA-A*01:01 allele in the third wave and demonstrate the unique properties
30 of this allele. Thus, HLA-A*01:01-binding immunodominant epitopes are mostly derived from
31 ORF1ab. A set of epitopes from ORF1ab was tested, and their high immunogenicity was
32 confirmed. Moreover, analysis of the results of single-cell phenotyping of T-cells in recovered
33 patients showed that the predominant phenotype in HLA-A*01:01 carriers is central memory
34 T-cells. The predominance of T-lymphocytes of this phenotype may contribute to forming
35 long-term T-cell immunity in carriers of this allele. Our results can be the basis for highly
36 effective vaccines based on ORF1ab peptides.

NOTE: This preprint reports new research that has not been certified by peer review and should not be used to guide clinical practice.

37 Introduction

38

39 The Delta variant of SARS-CoV-2 caused the third wave of the COVID-19 pandemic in mid-
40 2021 in many countries, including Russia (1). The surge in incidence was associated with the
41 high transmissibility of this strain compared to the alpha variant (2). The increase in
42 transmissibility mainly was due to the rise in the number of viral particles exhaled at the peak
43 of infection by an infected person (up to 6 times compared to the Alpha variant) (3). Aside
44 from the increased risk of hospitalization, the Delta variant also increases the risk of death in
45 unvaccinated COVID-19 patients (4).

46

47 In the Delta variant, 18 protein level mutations significantly changed the course of the disease
48 (5). Five were located in the Spike protein and significantly decreased the effectiveness of
49 humoral immunity formed either naturally (recovered patients) or after vaccination (6). In
50 addition, one of these mutations (D614G) increased the affinity of the receptor-binding
51 domain (RBD) of the Spike protein to the ACE2 receptor (7). Finally, it should be noted that
52 the rate of virus replication has also changed: the Delta variant replicates two times slower
53 than the Alpha variant in the first 8 hours after infection *in vitro* (8). This circumstance is
54 crucial since the non-structural protein ORF8 produced by SARS-CoV-2 can directly interact
55 with major histocompatibility complex class I (MHC-I) molecules and suppress their
56 maturation. As a result, the export of MHC-I molecules to an infected cell's surface almost
57 wholly stops after 18 hours of ORF8 expression (9).

58

59 MHC-I molecules are one of the key mediators of the first steps of a specific immune response
60 to COVID-19. Right after entering a cell, SARS-CoV-2 induces the translation of its proteins.
61 Some of these proteins enter the proteasomes of the infected cell, become cleaved to short
62 peptides (8–12 amino acid residues), and bind to MHC-I molecules. After binding, the complex
63 consisting of the MHC-I molecule and the peptide is transferred to the infected cell's surface,
64 where it can interact with the T-cell receptor (TCR) of CD8+ T-cell from the central memory
65 or the effector memory subpopulations. In response to the interaction, the CD8+ T-
66 lymphocyte activates and destroys the infected cell using perforins and serine proteases (10).
67 The crucial role of long-term CD8+ T-cell activation in the immune response to COVID-19 has
68 been recently studied in a cohort of patients with different severity of disease (11,12).

69

70 There are three main types of MHC-I molecules encoded by HLA-A, HLA-B, and HLA-C genes.
71 Each gene is presented in two variants (alleles) inherited from parents. There exist dozens of
72 HLA alleles, and every allele encodes an MHC-I molecule with an individual ability to recognize
73 various self- and non-self-antigens (13). Individual combinations of HLA class I alleles
74 essentially affect the severity of multiple infectious diseases, including malaria (14),
75 tuberculosis (15), HIV (16), and viral hepatitis (13). Previously we have demonstrated the
76 important role of MHC-I peptide presentation in the development of a specific immune
77 response to the Wuhan-Hu-1 variant (GISAID accession EPI_ISL_402125) (17).

78

79 Over more than two years of the COVID-19 pandemic, the scientific community accumulated
80 a significant amount of information on the actual epitopes of various SARS-CoV-2 variants
81 (18), features of the formation of T-cell memory (19), trends in the frequency of mutations in
82 the virus (20). However, the associations of the HLA genotypes and the course of COVID-19
83 were mainly analyzed according to data related to the first wave of the pandemic and the

84 initial virus variant (21–24). Moreover, in studies of the associations between the severity of
85 COVID-19 and HLA-I genotypes, the age of the recovered patients was practically not
86 considered. It should be noted that age is a significant factor in the immune response to
87 COVID-19 (25–27). In particular, it has been shown that in people over 60 years of age,
88 telomere lengths of naïve T-lymphocytes decrease significantly, which leads to an almost 10-
89 fold drop in their ability to divide upon activation (28). Also, the T-cell receptor (TCR)
90 repertoire is reduced in older people (29).

91

92 Previously, in a cohort of the first wave of COVID-19 patients, we showed that the low number
93 of peptides presented by an individual's HLA-I genotype significantly correlates with COVID-
94 19 severity only in patients under the age of 60 (17). In this study, we compared the features
95 of the HLA-I genotypes of COVID-19 patients under 60 between the first and the third waves.
96 In addition, we assessed the influence of mutations in the SARS-CoV-2 variants on the
97 immunogenic epitopes of CD8+ T-lymphocytes.

98

99 Materials and methods

100

101 Design and Participants

102

103 Three groups of patients were enrolled in the study. First, the control group of 428 volunteers
104 was established using electronic HLA genotype records of the Federal Register of Bone
105 Marrow Donors (Pirogov Russian National Research Medical University) (17). The group of
106 147 patients of the first wave of COVID-19 was formed from May to August 2020 (Wave 1
107 group). Out of them, the subset of 28 COVID-19 convalescent donors of the first wave was
108 enrolled in a prospective trial (CPS group). Finally, the group of patients of the third wave was
109 formed from June to July 2021 (Wave 3 group). 219 COVID-19 patients in Wave 3 group
110 enrolled in O.M. Filatov City Clinical Hospital, (Moscow, Russia).

111

112 All patients had at least one positive test result for SARS-CoV-2 by reverse transcription PCR
113 (RT-qPCR) from nasopharyngeal swabs or bronchoalveolar lavage. Patients with pathologies
114 that led to greater morbidity or who had additional immunosuppression (patients with
115 diabetes, HIV, active cancer in treatment with chemotherapy, immunodeficiency,
116 autoimmune diseases with immunosuppressants, and transplants) were not included in the
117 study. The medical practitioner collected blood (2 ml) in ethylenediaminetetraacetic acid
118 (EDTA) tube for HLA genotyping.

119

120 The severity of the disease was defined according to the classification scheme used by the US
121 National Institutes of Health (from www.covid19treatmentguidelines.nih.gov): asymptomatic
122 (lack of symptoms), mild severity (fever, cough, muscle pain, but without respiratory difficulty
123 or abnormal chest imaging) and moderate/severe (lower respiratory disease at CT scan or
124 clinical assessment, oxygen saturation (SaO₂) > 93% on room air, but lung infiltrates less than
125 50%).

126

127 The study protocol was reviewed and approved by the Local Ethics Committee at the Pirogov
128 Russian National Research Medical University (Meeting No. 194 of March 16, 2020, Protocol
129 No. 2020/07), by the Local Ethics Committee at O.M. Filatov City Clinical Hospital (Protocol

130 No. 237 of June 25, 2021), and by the National Research Center for Hematology ethical
131 committee (N 150, 02.07.2020); the study was conducted in accordance with the Declaration
132 of Helsinki.

133

134 [Human Leukocyte Antigen Class I Genotyping With Targeted Next-Generation](#) 135 [Sequencing](#)

136

137 Genomic DNA was isolated from the frozen collected anticoagulated whole blood samples
138 using the QIAamp DNA Blood Mini Kit (QIAGEN GmbH, Hilden, Germany). HLA genotyping was
139 performed with the HLA-Expert kit (DNA Technology LLC, Russia) by amplifying exons 2 and 3
140 of the HLA-A/B/C genes and exon 2 of the HLA-DRB1/3/4/5/DQB1/DPB1 genes. Prepared
141 libraries were run on Illumina MiSeq sequencer using a standard flow-cell with 2x250 paired-
142 end sequencing. Reads were analyzed using HLA-Expert Software (DNA-Technology LLC,
143 Russia) and the IPD-IMGT/HLA database 3.41.0 (30).

144

145 HLA-genotyping of convalescent donors was performed using the One Lambda ALLType kit
146 (Thermo Fisher Scientific, USA), which uses multiplex PCR to amplify full HLA-A/B/C gene
147 sequences, and from exon 2 to the 30 UTR of the HLA525 DRB1/3/4/5/DQB1 genes as
148 described previously (11). Prepared libraries were run on Illumina MiSeq sequencer using a
149 standard flow-cell with 2x150 paired-end sequencing. Reads were analyzed using One
150 Lambda HLA TypeStream Visual Software (TSV), version 2.0.0.27232, and the IPD IMGT/HLA
151 database 3.39.0.0 (30). Processed genotype data are available in Supplementary Table S1.

152

153 [Peripheral blood mononuclear cell \(PBMC\) isolation](#)

154

155 30 mL of venous blood from CPS group donors was collected into EDTA tubes (Sarstedt) and
156 subjected to Ficoll (Paneco) density gradient centrifugation (400 x g, 30 min). Isolated PBMCs
157 were washed with PBS containing 2 mM EDTA and used for assays or frozen in fetal bovine
158 serum containing 7% DMSO.

159

160 [T-cell expansion](#)

161

162 Full details of the T-cell expansion are provided in the manuscript (11). Briefly, PBMCs
163 sampled from COVID-19 convalescents were expanded for 12 days with the pre-selected 94
164 SARS-CoV-2 peptides (final concentration of each = 10 μ M). On days 10 and 11, an aliquot of
165 cell suspension was used for anti-IFN- γ ELISA aiming at the identification of responses to
166 individual peptides.

167

168 [Cell stimulation with individual peptides](#)

169

170 After 10 days of expansion, an aliquot of cell culture was washed twice in 1.5 mL of PBS and
171 was then transferred to AIM-V medium (Thermo Fisher Scientific), plated at 1×10^5 cells per
172 well in 96-well plates, and incubated overnight (12–16 hours) with the smaller pools of
173 peptides, spanning the composition of the initial peptide set. The following day the culture
174 medium was collected and tested for IFN- γ as described below. If the cells reacted positively
175 to one or several pools we sampled an aliquot of cell culture again on days 11–12, and

176 stimulated it as described above individually with each peptide (2 μ M) from those peptide
177 pools. Only peptides predicted to bind to each individual's HLA were tested.

178

179 Anti-IFN- γ ELISA

180

181 Culture 96-well plates with cells, incubated with peptide pools or individual peptides were
182 centrifuged for 3 minutes at 700g, and 100 μ L of the medium was transferred to the ELISA
183 plates and the detection of IFN- γ was performed (11). OD was measured at 450 nm on a
184 MultiScan FC (Thermo Fisher Scientific) instrument (OD450).

185

186 Test wells (medium from cells, incubated with peptides) were compared with negative control
187 wells (cells incubated with the solvent for peptides). Test wells with the ratio
188 OD450_test_well/OD450_negative control \geq 1.25 and the difference OD450_test_well –
189 OD450_negative control \geq 0.08 were considered positive. Peptides with a ratio between 1.25
190 and 1.5 were tested again up to 3 times as biological replicates to ensure the accuracy of their
191 response, and peptides with 2 or 3 positive results were considered positive.

192

193 Peptides

194

195 Peptides (at least 95% purity) were synthesized either by Peptide 2.0 Inc. or by the Shemyakin-
196 Ovchinnikov Institute of Bioorganic Chemistry RAS.

197

198 Assessing immunodominant epitopes for HLA-A*01:01 and HLA-A*02:01 and mutations 199 in VOC

200

201 To assess the immunodominant epitopes of HLA-A*01:01 and HLA-A*02:01, we queried IEDB
202 (18) for epitopes with positive MHC binding and positive T-cell assays using "Severe acute
203 respiratory syndrome-related coronavirus" as "Organism" on May 17, 2022. Epitopes with
204 more than 50% response rate for the respective allele carriers were considered
205 immunodominant. Mutation analysis was performed using data extracted from T-cell COVID-
206 19 Atlas (20) (accessed May 30, 2022) and included 16 VOC strains.

207

208 Phenotype analysis of CD8+ T-lymphocytes of convalescent HLA-A*01:01 and HLA- 209 A*02:01 alleles carriers

210

211 The data were obtained from supplementary materials of Francis et al. (19). The experiment
212 conducted by the authors consisted in performing single-cell RNA sequencing (scRNA-seq) of
213 T-cells bound to DNA-barcoded peptide-HLA tetramers. This approach allowed us to extract
214 information on both TCR sequences and their specific HLA-epitope pairs. Francis with
215 coauthors used a comprehensive library of SARS-CoV-2 epitopes and epitopes emerging from
216 SARS-CoV-1, cytomegalovirus, Epstein-Barr virus, and influenza. For the analysis of the
217 distribution of epitopes across the SARS-CoV-2 genome, the data file S3 was used. It includes
218 the list of SARS-CoV-2 reactive clonotypes with their specific epitopes and their antigen
219 source. In addition, the list of SARS-CoV-2 epitopes was extracted, and duplicate entries were
220 removed.

221

222 The data file S7 was used for the analysis of the T-cell phenotypes. It comprises the
223 information about the phenotypes of T-cells reacting to particular epitopes. The phenotypes
224 of T-cells were computationally assigned by the authors based on the analysis of differentially
225 expressed genes. The authors note that they identified several distinct cell clusters, but
226 except for naïve cells, central memory, and fully activated cytotoxic effectors, all other
227 clusters had mixed properties, making it impossible to determine their phenotypes univocally.
228 Therefore, we decided to take only the definitely determined cell phenotypes into our
229 analysis: naïve cells, central memory, and fully activated cytotoxic effector cells.

230

231 [Bioinformatics analysis of HLA/peptide interactions](#)

232

233 Protein sequences of SARS-CoV-2 variants were obtained from GISAID portal (Elbe &
234 Buckland-Merrett, 2017): EPI_ISL_402125 (Wuhan), EPI_ISL_1663516 (Delta, B.1.617.2),
235 EPI_ISL_6699752 (Omicron BA.1, B.1.1.529), EPI_ISL_9884589 (Omicron BA.2, B.1.1.529),
236 EPI_ISL_9854919 (Omicron BA.3, B.1.1.529), EPI_ISL_11873073 (Omicron BA.4, B.1.1.529).
237 T-CoV pipeline was executed to analyze HLA/peptide interactions (5,20). In the pipeline's
238 core, binding affinities of all viral peptides and 169 frequent HLA class I molecules were
239 predicted using NetMHCpan 4.1 (31).

240

241 [Statistical Analysis](#)

242 Allele frequencies in considered cohorts were estimated by dividing the number of
243 occurrences of a given allele in individuals by the doubled total number of individuals (i.e.,
244 identical alleles of homozygous individuals were counted as two occurrences). The following
245 functions from the stats library in R were used to conduct statistical testing: `fisher.test` for
246 Fisher's exact test, `wilcox.test` for Mann-Whitney U test. In addition, the Benjamini-Hochberg
247 procedure was used to perform multiple testing corrections. Plots were constructed with
248 `ggpubr` and `heatmap` libraries.

249

250

251 Results

252

253 Distribution of HLA Class I Alleles in the cohorts of patients of the first and the third 254 waves of COVID-19

255

256 We performed HLA class I genotyping of 147 patients who tested positive for COVID-19 during
257 the first wave of COVID-19 in Moscow (from May to August 2020, Wave 1 group). Also, 219
258 COVID-19 patients were genotyped from June to July 2021 (Wave 3 group). The demographic
259 and clinical data of these groups are summarized in Table 1. We did not find significant
260 differences in the age of patients in the comparison groups and the gender ratio in the groups.
261 The fraction of vaccinated patients (two doses of Sputnik V vaccine) in the Wave 3 group was
262 insignificant and equal to 8.7%, slightly lower than the citywide vaccination rate for June 2021
263 – 15% (32). There was a significant increase in the proportion of patients with obstructive
264 pulmonary disease (Fisher's exact test $p = 0.01$), obesity (Fisher's exact test $p = 0.01$, OR =
265 3.8), hypertension (Fisher's exact test $p = 0.003$, OR = 2.4) in the third wave of COVID-19. We
266 also assessed the contribution of comorbidities to the risk of death from COVID-19.
267 Interestingly, heart disease hypertension (Fisher's exact test $p = 5.2e-5$, OR = 13) and
268 hypertension (Fisher's exact test $p = 0.045$, OR = 3.5) were significant death risk factors in the
269 first wave. At the same time, no similar effects were observed for the third wave patients
270 (Supplementary Table S2).

271

272

273 **Table 1. Characteristics of participants by groups.**

	Wave 1	Wave 3	p-value
n	147	219	
Age	43.4 +/- 11	42.9 +/- 5.2	0,4
Sex			
male	73 (49.7%)	123 (56.2%)	0,24, OR = 0.77
female	74 (50.3%)	96 (43.8%)	
Vaccination	0	19 (8.7%)	4.9e-05
Severity			
mild/moderate	120 (81.6%)	192 (87.7%)	0.13, OR = 0.63
severe	27 (18.4%)	27 (12.3%)	
Outcome			
recovered	127 (86.4%)	197 (90%)	0.32, OR = 0.71
deceased	20 (13.6%)	22 (10%)	
ICU	28 (19%)	51 (23.3%)	0.36, OR = 1.3
Oxygen support			
non	98 (66.7%)	140 (63.9%)	
low flow nasal oxygen supplementation	24 (16.3%)	38 (17.4%)	
prone position	0	11 (5%)	8.8e-05
high-flow oxygen therapy	16 (10.9%)	4 (1.8%)	
mechanical ventilation	9 (6.1%)	26 (11.9%)	
Obstructive pulmonary disease	0	9 (4.1%)	0.01, OR = inf
Obesity	4 (2.7%)	21 (9.6%)	0.01, OR = 3.8
Heart diseases	20 (9.1%)	14 (9.5%)	1, OR = 0.95
Hypertension	16 (10.9%)	50 (22.8%)	0.003, OR = 2.4
Neoplasma	3 (2%)	9 (4.1%)	0.4, OR = 2.1

274

275

276 First, we tested whether the frequency of a single allele can differentiate individuals from
277 three groups: COVID-19 patients of the first wave, COVID-19 patients of the third wave, and

278 the control group. The distribution of major HLA-A, HLA-B, and HLA-C alleles in these three
279 groups is summarized in Figure 1. Fisher's exact test was used to make formal statistical
280 comparisons. As a result, we found that for all possible group comparisons, only one allele
281 out of dozen top alleles had a high odds ratio, which can be considered statistically significant
282 after multiple testing correction. Specifically, frequency of HLA-A*01:01 allele decreased from
283 17.3% in the Wave 1 group to 9.8% in the Wave 3 group (Fisher's exact test adj.p = 0.025, OR
284 = 0.5). Some of the alleles were differentially enriched if no multiple testing correction was
285 applied (Supplementary Table S3).

286
287 We hypothesized that the decrease in the frequency of HLA-A*01:01 carriers among patients
288 of the third wave group could be attributed to the characteristics of the T-cell response. To
289 test this hypothesis, computational methods were used to analyze the interactions between
290 the HLA-I molecules and the viral peptides, the effects of mutations in variants of concern
291 (VOC) on these interactions, as well as the results of experimental testing of the
292 immunogenicity of peptides in patients who recovered from the COVID-19 in the first wave.

293
294 [Analysis of the binding affinity of SARS-CoV-2 peptides with MHC-I molecules](#)
295 We predicted the number of viral peptides presented by the 12 most common alleles in the
296 European population (33) (Figure 2). The ability of HLA-A*01:01 to interact with peptides of
297 both structural and non-structural proteins of the virus was moderate. Namely, it was
298 predicted to interact with an affinity of less than 50 nM (tightly binding peptides) with 28
299 peptides from ORF1ab and 8 peptides from structural and accessory proteins. Another allele,
300 HLA-A*02:01, was the most frequent in the population and had 207 predicted tight binders
301 from ORF1ab and 56 tight binders from the other proteins. We also compared the ability to
302 present viral peptides between genotypes that include HLA-A*01:01 and genotypes which do
303 not include this allele (Figure S1). HLA-I genotypes, which included HLA-A*01:01, had, on
304 average, a lower number of high-affinity peptides compared to non-carriers regardless of
305 wave (Mann-Whitney U test $p < 0.02$).

306
307 [Analysis of immunogenic epitopes](#)
308 Next, we analyzed the immunogenic epitopes of SARS-CoV-2 using the data from the IEDB
309 portal for HLA-A*01:01 and HLA-A*02:01 alleles. At the time of the analysis (May 2022), the
310 database contained information on the T-cell responses to 365 viral peptides. Two common
311 epitopes were found for both alleles: CNDPFLGVY (S protein), VATSRTLSTY (M protein). For the
312 HLA-A*01:01 allele, the immunogenicity of 50 ORF1ab peptides and 33 non-ORF1ab peptides
313 was validated. In entire agreement with computational predictions, the number of epitopes
314 was higher for the HLA-A*02:01 allele: 139 ORF1ab peptides and 145 non-ORF1ab peptides.
315 The ratio of peptides from ORF1ab for the HLA-A*01:01 allele was 1.6 times higher than for
316 the HLA-A*02:01 allele (Fisher's Exact Test p-value = 0.08). Among the tested peptides,
317 immunodominant epitopes were identified (i.e., caused a response of T-lymphocytes in at
318 least 50% of the tested samples). For the HLA-A*01:01 allele, 10 immunodominant epitopes
319 from ORF1ab and only 3 epitopes not from ORF1ab were identified. For the HLA-A*02:01
320 allele, 51 immunodominant epitopes from ORF1ab and 59 from non-ORF1ab were identified.
321 The ratio of immunodominant epitopes from ORF1ab for the HLA-A*01:01 allele was 3.8 times
322 higher than for the HLA-A*02:01 allele (Fisher's Exact Test p-value = 0.04).

323

324 Validation of ORF1ab epitopes in a subset of convalescent HLA-A*01:01 and HLA- 325 A*02:01 carriers

326 To validate the hypothesis that the first wave convalescent HLA-A*01:01 allele carriers had a
327 high number of immunogenic epitopes from ORF1ab proteins, we analyzed the T-cell
328 responses of 28 first wave convalescent patients who carried the two most common alleles
329 in the European population: HLA-A*01:01 (13 patients) and HLA-A*02:01 (15 patients).
330 Individual immunogenicity of 15 validated epitopes from SARS-CoV-2 ORF1ab
331 (Supplementary Table S4) was tested for each T-cell sample. The peptides from this panel did
332 not induce a T-cell response in patients who had not previously had COVID-19 (11). The
333 number of epitopes for HLA-A*01:01 was 7 for HLA-A*02:01 – 8.

334
335 To exclude the possibility of influence on the strength of the T-cell response, the time from
336 the onset of symptoms of the disease to the time of the analysis, we compared this parameter
337 between groups. For HLA-A*01:01 carriers, the median time after symptoms onset was 34
338 days, and for HLA-A*02:01 carriers, it was 41 days; the differences were insignificant (Figure
339 3A). At the same time, the true positive rates for these alleles differed significantly for
340 epitopes from ORF1ab (Figure 3B). Three of the 7 HLA-A*01:01 epitopes tested were
341 immunodominant (TTDPSFLGRY, HTTDPFLGRY, PTDNYITTY), but there were no
342 immunodominant epitopes out of 8 tested for HLA-A*02:01.

343

344 Phenotype analysis of CD8+ T-lymphocytes of convalescent patients

345 Aside from IEDB and own epitope validation data, we analyzed *ex vivo* scRNA-seq data of
346 convalescent individuals CD8+ T-cells activated by single peptides (19). The considered
347 dataset included the set of phenotyped T-cell clones responding to a comprehensive set of
348 SARS-CoV-2 derived epitopes associated with four major HLA class I alleles (HLA-A*01:01,
349 HLA-A*02:01, HLA-A*24:02, and HLA-B*07:02). First, we examined the distribution of SARS-
350 CoV-2 derived epitopes which elicited T-cell response according to the genomic region from
351 which they originated. Concordantly with the results mentioned above, the majority of HLA-
352 A*01:01 epitopes were from ORF1ab. The same tendency was not observed for the other
353 alleles (Figure 4A).

354
355 Next, we analyzed the phenotypes of responding T-cell clones (Figure 4B). HLA-A*01:01-
356 associated epitopes elicited responses mainly from the Tcm subpopulation. At the same time,
357 the proportion of Tcm responding cells for other alleles was significantly smaller (Fisher Exact
358 Test pairwise comparisons of A*01:01 with A*02:01, B*07:02, and A*24:02 results in p-values
359 < 0.02). Together with the observation that most of the known HLA-A*01:01-associated
360 epitopes originated from the conservative ORF1ab region, these results imply that people
361 bearing HLA-A*01:01 may have a higher chance of eliciting robust immune response upon
362 secondary exposure to SARS-CoV-2 due to the pre-existing immune memory.

363

364 Analysis of the mutations in the VOC on CD8+ epitopes

365 Then, we analyzed the changes in the affinity of the interactions of immunodominant
366 epitopes with HLA-A*01:01 and HLA-A*02:01 induced by mutations in VOCs, including the
367 Delta variant. Strikingly, none of the HLA-A*01:01 immunodominant epitopes were affected
368 by mutations in the current VOCs: Delta G/478K.V1 and Omicron (BA.1 – BA.4). At the same
369 time, seven HLA-A*02:01 immunodominant epitopes were affected by the mutations. Six
370 were located in the Spike protein and one in the NS3 protein. All except one mutation led to

371 the decrease in the affinity of the interaction with HLA-A*02:01. Specifically, in Omicron BA.1
 372 the YGFQPTNGV peptide from Spike protein had three substitutions (G496S, Q498R, N501Y),
 373 which resulted in an increase in the affinity of its interaction with HLA-A*02:01 (from 2160
 374 nM to 87 nM). In VOC Omicron BA.1 and BA.3, A67V and HV 69-70 deletion mutations resulted
 375 in the disappearance of the immunodominant epitope VTWFHAIHV from the Spike protein.

376
 377 In addition, the effect of mutations in the VOCs on the affinity of the interactions of all
 378 possible viral peptides with the 12 abovementioned HLA-I alleles was analyzed (Table 2). HLA-
 379 A*01:01 had 51 high-affinity peptides from ORF1ab and 13 high-affinity peptides from other
 380 proteins (structural and accessory) for the Wuhan-Hu-1 strain. A distinctive feature of this
 381 allele was that it had a relatively high number of high-affinity peptides, although VOC
 382 mutations do not affect them (Figure 5). Of the 64 high-affinity HLA-A*01:01 peptides, only
 383 one peptide significantly changed the affinity in 16 VOCs analyzed. At the same time, similar
 384 to the number of tight binders allele HLA-A*24:02 had 27 altered peptides from ORF1ab
 385 (Fisher's exact test p-value = 3e-09, OR = 0.02). It should be noted that the high-affinity
 386 peptides from ORF1ab for all analyzed alleles were less affected by the mutations compared
 387 to the rest of the peptides (Mann-Whitney U test p-value = 0.05).

388

389 **Table 2. The number of high-affinity peptides mutated in VOCs.**

Allele	Frequency in study population	Total number of changed non ORF1ab tight binders in all VOC	Total number of changed ORF1ab tight binders in all VOC	Number of non ORF1ab tight binders in Wuhan-Hu-1	Number of ORF1ab tight binders in Wuhan-Hu-1
HLA-A*02:01	25.44	67	146	96	305
HLA-A*03:01	12.97	34	31	29	100
HLA-C*12:03	12.78	40	4	32	72
HLA-A*01:01	13.1	1	0	13	51
HLA-A*24:02	11.34	22	5	17	46
HLA-B*07:02	9.89	47	27	16	39
HLA-B*08:01	7.24	5	15	12	29
HLA-B*18:01	7.24	10	0	7	25
HLA-C*07:02	11.71	0	0	1	10
HLA-C*06:02	10.96	0	2	1	5
HLA-C*07:01	12.03	0	0	0	2
HLA-C*04:01	12.41	0	0	0	0

390

391 Discussion

392

393 We conducted a comparative study of the HLA-I genotypes of symptomatic COVID-19 patients
 394 of the pandemic's first and third waves. Genotypes of 147 patients (first wave) and 219 (third
 395 wave) were studied. We found a significant increase in the proportion of patients with
 396 obstructive pulmonary disease, obesity, and hypertension in the third wave of COVID-19. This

397 circumstance may be associated not only with the peculiarities of the Delta variant but also
398 with the possible population's fatigue from complying with anti-epidemic measures, which
399 led to the infection of risk groups that previously more strictly kept the social distancing
400 regime (34).

401
402 We tested whether the frequency of HLA alleles can differentiate individuals from three
403 groups: COVID-19 patients of the first wave, COVID-19 patients of the third wave, and the
404 control group. We found that for all possible group comparisons, only one allele out of the
405 most abundant alleles had a statistically significant odds ratio after multiple testing
406 correction. Namely, the frequency of the HLA-A*01:01 allele in the Wave 3 group fell by half
407 relative to the Wave 1 group. Previously, the HLA-A*01:01 allele was considered a risk allele
408 for infection and severe course of COVID-19 in the first wave (17,35–37). At the same time,
409 the protective role of this allele against the formation of Severe Bilateral Pneumonia caused
410 by COVID-19 was also reported (38).

411
412 We suggested that the decrease in the frequency of HLA-A*01:01 carriers among patients of
413 the third wave could be associated with the characteristics of the previously formed T-cell
414 responses. It is known that up to 50% of cases of COVID-19 are asymptomatic (39,40) and lead
415 to the formation of neutralizing antibodies and multispecific T-cells (41). While the efficiency
416 of neutralizing antibodies decreases for VOCs (42), the formed pool of multispecific T-cells in
417 most cases can provide an immune response regardless of viral mutations (5).

418
419 To test this hypothesis, we first analyzed the number of viral peptides interacting with the 12
420 most common alleles in the European population with bioinformatics methods. HLA-A*01:01
421 allele was one of the alleles with a moderate ability to interact with peptides of both structural
422 and non-structural proteins of the virus. We also found that HLA-A*01:01 carriers have fewer
423 predicted high-affinity peptides compared to the non-carriers, regardless of the wave of
424 COVID-19.

425
426 Analysis of the confirmed immunogenic epitopes of SARS-CoV-2 according to the IEDB
427 database showed that 10 immunodominant epitopes from ORF1ab and only 3 not from
428 ORF1ab were identified for HLA-A*01:01. In turn, there were 51 immunodominant epitopes
429 from ORF1ab and 59 epitopes not from ORF1ab for the HLA-A*02:01 allele. Thus, the ratio of
430 immunodominant epitopes from ORF1ab for the HLA-A*01:01 allele was 3.8 times greater
431 than for the HLA-A*02:01 allele. We additionally validated these data by analyzing the T-cell
432 responses of 28 carriers HLA-A*01:01 and HLA-A*02:01 alleles. Concordantly with IEDB data,
433 the true positive rates for ORF1ab epitopes were significantly higher for HLA-A*01:01
434 compared to the HLA-A*02:01. One of the possible explanations for these data may be the
435 higher proportion of formed central memory CD8⁺ T-cells in HLA-A*01:01 carriers compared
436 to the A*02:01, B*07:02, and A*24:02 carriers.

437
438 Moreover, an ORF1ab-derived HLA-A*01:01-restricted epitope TTDPFSFLRGY was shown in
439 multiple studies to induce exceptionally high frequency of T-cells (magnitude of response) in
440 comparison to other multiple immunodominant epitopes (43–46). Furthermore, it was shown
441 that the response of PBMCs of HLA-A*01:01⁺ convalescents to the epitopes derived from non-
442 structural proteins was higher than to the structural proteins. This was not observed for HLA-

443 A*01:01⁻ convalescents (11). This further suggests high importance of ORF1ab-focused T-cell
444 response for carriers of HLA-A*01:01.

445

446 Not a single immunodominant HLA-A*01:01 epitope significantly changed its presentation
447 affinity due to mutations in the actual VOCs: Delta G/478K.V1, Omicron (BA.1 – BA. 4). At the
448 same time, other alleles such as HLA-A*02:01 were affected by the mutations. Interestingly,
449 HLA-A*01:01 was the only allele with a relatively high number of high-affinity peptides
450 unaffected by the mutations. In agreement with the reports on the lower mutation rate in
451 ORF1ab (47), high-affinity peptides from ORF1ab for all analyzed alleles were less affected by
452 mutations compared to the rest of the proteins.

453

454 This study demonstrates for the first time the possibility of HLA-A*01:01 allele vanishment
455 between the cohorts of symptomatic COVID-19 patients from different waves. Furthermore,
456 the discovered characteristics of peptide presentation by HLA-A*01:01 could be important
457 for developing vaccines to induce T-cell responses.

458

459 References

460

- 461 1. Klink G v, Safina KR, Nabieva E, Shvyrev N, Garushyants S, Alekseeva E, Komissarov AB,
462 Danilenko DM, Pochtovyi AA, Divisenko E v, et al. The rise and spread of the SARS-CoV-
463 2 AY.122 lineage in Russia. *Virus Evolution* (2022) 8: doi: 10.1093/ve/veac017
- 464 2. Callaway E. Delta coronavirus variant: scientists brace for impact. *Nature* (2021)
465 595:17–18. doi: 10.1038/d41586-021-01696-3
- 466 3. Earnest R, Uddin R, Matluk N, Renzette N, Turbett SE, Siddle KJ, Loreth C, Adams G,
467 Tomkins-Tinch CH, Petrone ME, et al. Comparative transmissibility of SARS-CoV-2
468 variants Delta and Alpha in New England, USA. *Cell Reports Medicine* (2022) 3:100583.
469 doi: 10.1016/j.xcrm.2022.100583
- 470 4. Bast E, Tang F, Dahn J, Palacio A. Increased risk of hospitalisation and death with the
471 delta variant in the USA. *The Lancet Infectious Diseases* (2021) 21:1629–1630. doi:
472 10.1016/S1473-3099(21)00685-X
- 473 5. Nersisyan S, Zhiyanov A, Zakharova M, Ishina I, Kurbatskaia I, Mamedov A, Galatenko
474 A, Shkurnikov M, Gabibov A, Tonevitsky A. Alterations in SARS-CoV-2 Omicron and
475 Delta peptides presentation by HLA molecules. *PeerJ* (2022) 10:e13354. doi:
476 10.7717/peerj.13354
- 477 6. Bian L, Gao Q, Gao F, Wang Q, He Q, Wu X, Mao Q, Xu M, Liang Z. Impact of the Delta
478 variant on vaccine efficacy and response strategies. *Expert Review of Vaccines* (2021)
479 20:1201–1209. doi: 10.1080/14760584.2021.1976153
- 480 7. Ozono S, Zhang Y, Ode H, Sano K, Tan TS, Imai K, Miyoshi K, Kishigami S, Ueno T, Iwatani
481 Y, et al. SARS-CoV-2 D614G spike mutation increases entry efficiency with enhanced
482 ACE2-binding affinity. *Nature Communications* (2021) 12:848. doi: 10.1038/s41467-
483 021-21118-2
- 484 8. Shuai H, Chan JF-W, Hu B, Chai Y, Yuen TT-T, Yin F, Huang X, Yoon C, Hu J-C, Liu H, et al.
485 Attenuated replication and pathogenicity of SARS-CoV-2 B.1.1.529 Omicron. *Nature*
486 (2022) 603:693–699. doi: 10.1038/s41586-022-04442-5
- 487 9. Zhang Y, Chen Y, Li Y, Huang F, Luo B, Yuan Y, Xia B, Ma X, Yang T, Yu F, et al. The ORF8
488 protein of SARS-CoV-2 mediates immune evasion through down-regulating MHC-I.
489 *Proceedings of the National Academy of Sciences* (2021) 118: doi:
490 10.1073/pnas.2024202118
- 491 10. Wherry EJ, Ahmed R. Memory CD8 T-Cell Differentiation during Viral Infection. *Journal*
492 *of Virology* (2004) 78:5535–5545. doi: 10.1128/jvi.78.11.5535-5545.2004
- 493 11. Titov A, Shaykhutdinova R, Shcherbakova O v., Serdyuk Y v., Sheetikov SA, Zornikova K
494 v., Maleeva A v., Khmelevskaya A, Dianov D v., Shakirova NT, et al. Immunogenic
495 epitope panel for accurate detection of non-cross-reactive T cell response to SARS-CoV-
496 2. *JCI Insight* (2022) 7: doi: 10.1172/jci.insight.157699
- 497 12. Gattinger P, Borochova K, Dorofeeva Y, Henning R, Kiss R, Kratzer B, Mühl B, Perkmann
498 T, Trapin D, Trella M, et al. Antibodies in serum of convalescent patients following mild
499 COVID-19 do not always prevent virus-receptor binding. *Allergy* (2021) 76:878–883.
500 doi: 10.1111/all.14523
- 501 13. Wang JH, Zheng X, Ke X, Dorak MT, Shen J, Boodram B, O’Gorman M, Beaman K, Cotler
502 SJ, Hershov R, et al. Ethnic and geographical differences in HLA associations with the
503 outcome of hepatitis C virus infection. *Virology Journal* (2009) 6: doi: 10.1186/1743-
504 422X-6-46

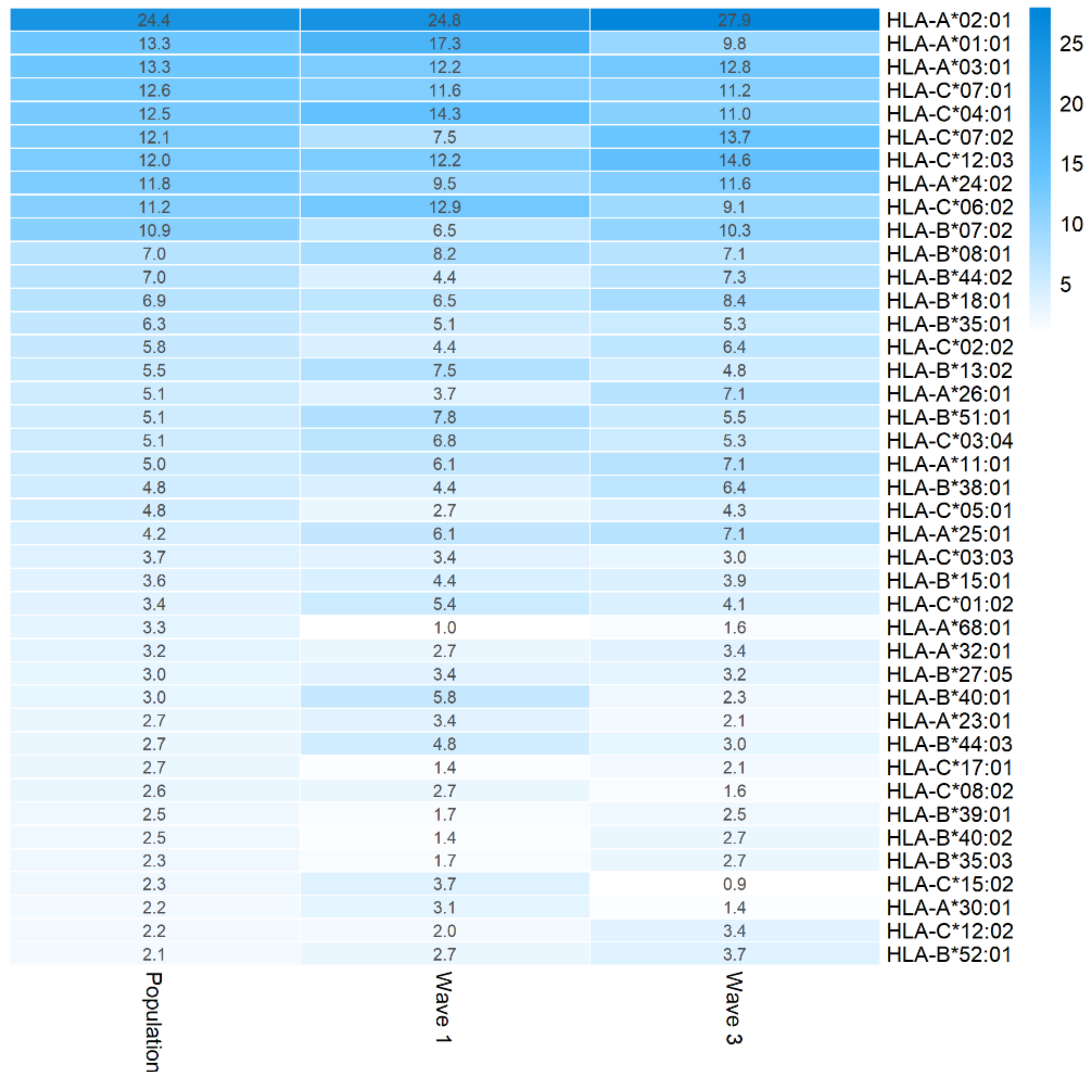
- 505 14. Lima-Junior J da C, Pratt-Riccio LR. Major histocompatibility complex and malaria:
506 Focus on Plasmodium vivax Infection. *Frontiers in Immunology* (2016) 7: doi:
507 10.3389/fimmu.2016.00013
- 508 15. Mazzaccaro RJ, Gedde M, Jensen ER, van Santen HM, Ploegh HL, Rock KL, Bloom BR.
509 Major histocompatibility class I presentation of soluble antigen facilitated by
510 Mycobacterium tuberculosis infection. *Proc Natl Acad Sci U S A* (1996) 93:11786–
511 11791. doi: 10.1073/pnas.93.21.11786
- 512 16. Goulder PJR, Watkins DI. Impact of MHC class I diversity on immune control of
513 immunodeficiency virus replication. *Nature Reviews Immunology* (2008) 8:619–630.
514 doi: 10.1038/nri2357
- 515 17. Shkurnikov M, Nersisyan S, Jankevic T, Galatenko A, Gordeev I, Vechorko V, Tonevitsky
516 A. Association of HLA Class I Genotypes With Severity of Coronavirus Disease-19.
517 *Frontiers in Immunology* (2021) 12:641900. doi: 10.3389/fimmu.2021.641900
- 518 18. Vita R, Mahajan S, Overton JA, Dhanda SK, Martini S, Cantrell JR, Wheeler DK, Sette A,
519 Peters B. The Immune Epitope Database (IEDB): 2018 update. *Nucleic Acids Research*
520 (2019) 47:D339–D343. doi: 10.1093/nar/gky1006
- 521 19. Francis JM, Leistritz-Edwards D, Dunn A, Tarr C, Lehman J, Dempsey C, Hamel A, Rayon
522 V, Liu G, Wang Y, et al. Allelic variation in class I HLA determines CD8+ T cell repertoire
523 shape and cross-reactive memory responses to SARS-CoV-2. *Sci Immunol* (2022)
524 7:eabk3070. doi: 10.1126/sciimmunol.abk3070
- 525 20. Nersisyan S, Zhiyanov A, Shkurnikov M, Tonevitsky A. T-CoV: a comprehensive portal
526 of HLA-peptide interactions affected by SARS-CoV-2 mutations. *Nucleic Acids Research*
527 (2022) 50:D883–D887. doi: 10.1093/nar/gkab701
- 528 21. Tavasolian F, Rashidi M, Hatam GR, Jeddi M, Hosseini AZ, Mosawi SH, Abdollahi E,
529 Inman RD. HLA, Immune Response, and Susceptibility to COVID-19. *Frontiers in*
530 *Immunology* (2021) 11: doi: 10.3389/fimmu.2020.601886
- 531 22. Lorente L, Martín MM, Franco A, Barrios Y, Cáceres JJ, Solé-Violán J, Perez A, Marcos y
532 Ramos JA, Ramos-Gómez L, Ojeda N, et al. HLA genetic polymorphisms and prognosis
533 of patients with COVID-19. *Medicina Intensiva* (2021) 45:96–103. doi:
534 10.1016/j.medin.2020.08.004
- 535 23. Langton DJ, Bourke SC, Lie BA, Reiff G, Natsu S, Darlay R, Burn J, Echevarria C. The
536 influence of HLA genotype on the severity of COVID-19 infection. *HLA* (2021) 98:14–22.
537 doi: 10.1111/tan.14284
- 538 24. Venet F, Gossez M, Bidar F, Bodinier M, Coudereau R, Lukaszewicz A-C, Tardiveau C,
539 Brengel-Pesce K, Cheynet V, Cazalis M-A, et al. T cell response against SARS-CoV-2
540 persists after one year in patients surviving severe COVID-19. *eBioMedicine* (2022)
541 78:103967. doi: 10.1016/j.ebiom.2022.103967
- 542 25. Promislow DEL. A Geroscience Perspective on COVID-19 Mortality. *The Journals of*
543 *Gerontology: Series A* (2020) 75:e30–e33. doi: 10.1093/gerona/glaa094
- 544 26. McGroder CF, Zhang D, Choudhury MA, Salvatore MM, D’Souza BM, Hoffman EA, Wei
545 Y, Baldwin MR, Garcia CK. Pulmonary fibrosis 4 months after COVID-19 is associated
546 with severity of illness and blood leucocyte telomere length. *Thorax* (2021) 76:1242–
547 1245. doi: 10.1136/thoraxjnl-2021-217031
- 548 27. Sanchez-Vazquez R, Guío-Carrión A, Zapatero-Gaviria A, Martínez P, Blasco MA. Shorter
549 telomere lengths in patients with severe COVID-19 disease. *Aging* (2021) 13:1–15. doi:
550 10.18632/aging.202463

- 551 28. Anderson JJ, Susser E, Arbeev KG, Yashin AI, Levy D, Verhulst S, Aviv A. Telomere-length
552 dependent T-cell clonal expansion: A model linking ageing to COVID-19 T-cell
553 lymphopenia and mortality. *eBioMedicine* (2022) 78:103978. doi:
554 10.1016/j.ebiom.2022.103978
- 555 29. Britanova O v., Putintseva E v., Shugay M, Merzlyak EM, Turchaninova MA, Staroverov
556 DB, Bolotin DA, Lukyanov S, Bogdanova EA, Mamedov IZ, et al. Age-Related Decrease
557 in TCR Repertoire Diversity Measured with Deep and Normalized Sequence Profiling.
558 *The Journal of Immunology* (2014) 192:2689–2698. doi: 10.4049/jimmunol.1302064
- 559 30. Robinson J, Barker DJ, Georgiou X, Cooper MA, Flicek P, Marsh SGE. IPD-IMGT/HLA
560 Database. *Nucleic Acids Research* (2020) 48:D948–D955. doi: 10.1093/nar/gkz950
- 561 31. Reynisson B, Alvarez B, Paul S, Peters B, Nielsen M. NetMHCpan-4.1 and NetMHCIIpan-
562 4.0: improved predictions of MHC antigen presentation by concurrent motif
563 deconvolution and integration of MS MHC eluted ligand data. *Nucleic Acids Res* (2020)
564 48:W449–W454. doi: 10.1093/nar/gkaa379
- 565 32. Boguslavsky D v., Sharova NP, Sharov KS. Public Policy Measures to Increase Anti-SARS-
566 CoV-2 Vaccination Rate in Russia. *International Journal of Environmental Research and
567 Public Health* (2022) 19:3387. doi: 10.3390/ijerph19063387
- 568 33. Gonzalez-Galarza FF, McCabe A, Santos EJM dos, Jones J, Takeshita L, Ortega-Rivera
569 ND, Cid-Pavon GM del, Ramsbottom K, Ghattaoraya G, Alfirevic A, et al. Allele
570 frequency net database (AFND) 2020 update: gold-standard data classification, open
571 access genotype data and new query tools. *Nucleic Acids Research* (2019) doi:
572 10.1093/nar/gkz1029
- 573 34. Chan EYY, Kim JH, Kwok K, Huang Z, Hung KKC, Wong ELY, Lee EKP, Wong SYS.
574 Population Adherence to Infection Control Behaviors during Hong Kong’s First and
575 Third COVID-19 Waves: A Serial Cross-Sectional Study. *International Journal of
576 Environmental Research and Public Health* (2021) 18:11176. doi:
577 10.3390/ijerph182111176
- 578 35. Pisanti S, Deelen J, Gallina AM, Caputo M, Citro M, Abate M, Sacchi N, Vecchione C,
579 Martinelli R. Correlation of the two most frequent HLA haplotypes in the Italian
580 population to the differential regional incidence of Covid-19. *Journal of Translational
581 Medicine* (2020) 18: doi: 10.1186/s12967-020-02515-5
- 582 36. Naemi FMA, Al-adwani S, Al-khatibi H, Al-nazawi A. Frequency of HLA alleles among
583 COVID-19 infected patients: Preliminary data from Saudi Arabia. *Virology* (2021) 560:1–
584 7. doi: 10.1016/j.virol.2021.04.011
- 585 37. Ishii T. Human Leukocyte Antigen (HLA) Class I Susceptible Alleles Against COVID-19
586 Increase Both Infection and Severity Rate. *Cureus* (2020) doi: 10.7759/cureus.12239
- 587 38. Suslova TA, Vavilov MN, Belyaeva S v, Evdokimov A v., Stashkevich DS, Galkin A, Kofiadi
588 IA. Distribution of HLA-A, -B, -C, -DRB1, -DQB1, -DPB1 allele frequencies in patients with
589 COVID-19 bilateral pneumonia in Russians, living in the Chelyabinsk region (Russia).
590 *Human Immunology* (2022) 83:547–550. doi: 10.1016/j.humimm.2022.04.009
- 591 39. Alene M, Yismaw L, Assemie MA, Ketema DB, Mengist B, Kassie B, Birhan TY. Magnitude
592 of asymptomatic COVID-19 cases throughout the course of infection: A systematic
593 review and meta-analysis. *PLOS ONE* (2021) 16:e0249090. doi:
594 10.1371/journal.pone.0249090
- 595 40. Byambasuren O, Cardona M, Bell K, Clark J, McLaws M-L, Glasziou P. Estimating the
596 extent of asymptomatic COVID-19 and its potential for community transmission:
597 Systematic review and meta-analysis. *Official Journal of the Association of Medical*

- 598 *Microbiology and Infectious Disease Canada* (2020) 5:223–234. doi: 10.3138/jammi-
599 2020-0030
- 600 41. Reynolds CJ, Swadling L, Gibbons JM, Pade C, Jensen MP, Diniz MO, Schmidt NM, Butler
601 DK, Amin OE, Bailey SNL, et al. Discordant neutralizing antibody and T cell responses in
602 asymptomatic and mild SARS-CoV-2 infection. *Science Immunology* (2020) 5: doi:
603 10.1126/sciimmunol.abf3698
- 604 42. Dupont L, Snell LB, Graham C, Seow J, Merrick B, Lechmere T, Maguire TJA, Hallett SR,
605 Pickering S, Charalampous T, et al. Neutralizing antibody activity in convalescent sera
606 from infection in humans with SARS-CoV-2 and variants of concern. *Nature*
607 *Microbiology* (2021) 6:1433–1442. doi: 10.1038/s41564-021-00974-0
- 608 43. Kared H, Redd AD, Bloch EM, Bonny TS, Sumatoh H, Kairi F, Carbajo D, Abel B, Newell
609 EW, Bettinotti MP, et al. SARS-CoV-2–specific CD8+ T cell responses in convalescent
610 COVID-19 individuals. *Journal of Clinical Investigation* (2021) 131: doi:
611 10.1172/JCI145476
- 612 44. Saini SK, Hersby DS, Tamhane T, Povlsen HR, Amaya Hernandez SP, Nielsen M, Gang
613 AO, Hadrup SR. SARS-CoV-2 genome-wide T cell epitope mapping reveals
614 immunodominance and substantial CD8+ T cell activation in COVID-19 patients. *Sci*
615 *Immunol* (2021) 6: doi: 10.1126/sciimmunol.abf7550
- 616 45. Gangaev A, Ketelaars SLC, Isaeva OI, Patiwaal S, Dopler A, Hoefakker K, de Biasi S,
617 Gibellini L, Mussini C, Guaraldi G, et al. Identification and characterization of a SARS-
618 CoV-2 specific CD8+ T cell response with immunodominant features. *Nat Commun*
619 (2021) 12:2593. doi: 10.1038/s41467-021-22811-y
- 620 46. Snyder TM, Gittelman RM, Klinger M, May DH, Osborne EJ, Taniguchi R, Zahid HJ,
621 Kaplan IM, Dines JN, Noakes MT, et al. Magnitude and Dynamics of the T-Cell Response
622 to SARS-CoV-2 Infection at Both Individual and Population Levels. *medRxiv* (2020) doi:
623 10.1101/2020.07.31.20165647
- 624 47. Vilar S, Isom DG. One Year of SARS-CoV-2: How Much Has the Virus Changed? *Biology*
625 *(Basel)* (2021) 10:91. doi: 10.3390/biology10020091
626
627

1 Figures

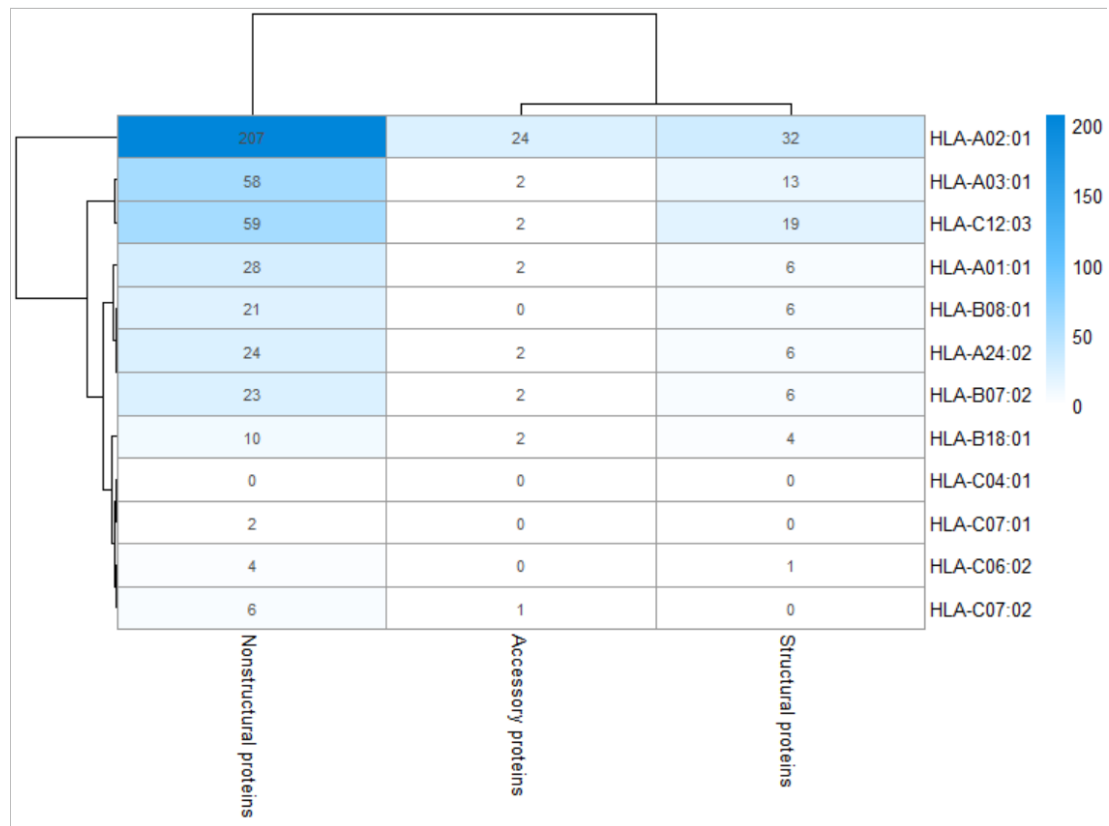
2



3

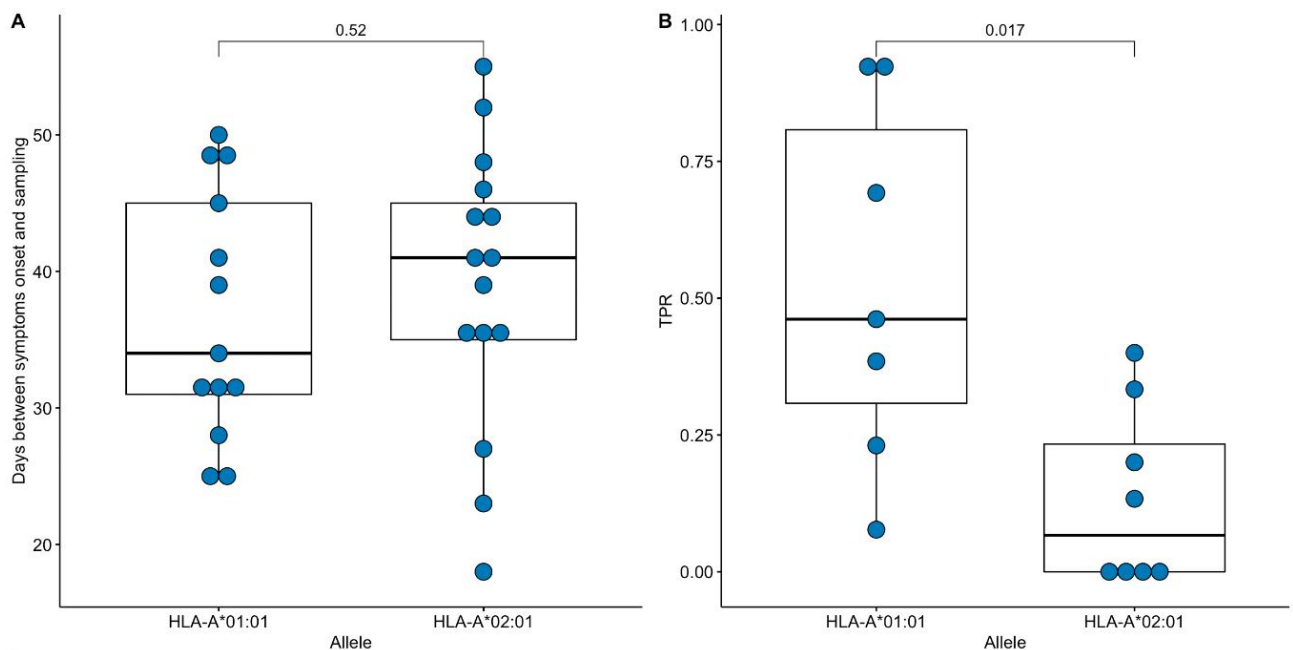
4

5 **Figure 1. Distribution of HLA-A, HLA-B, and HLA-C allele frequencies in the groups of COVID-**
 6 **19 patients and the control group. Alleles with frequency over 5% in at least one of three**
 7 **considered groups are presented.**

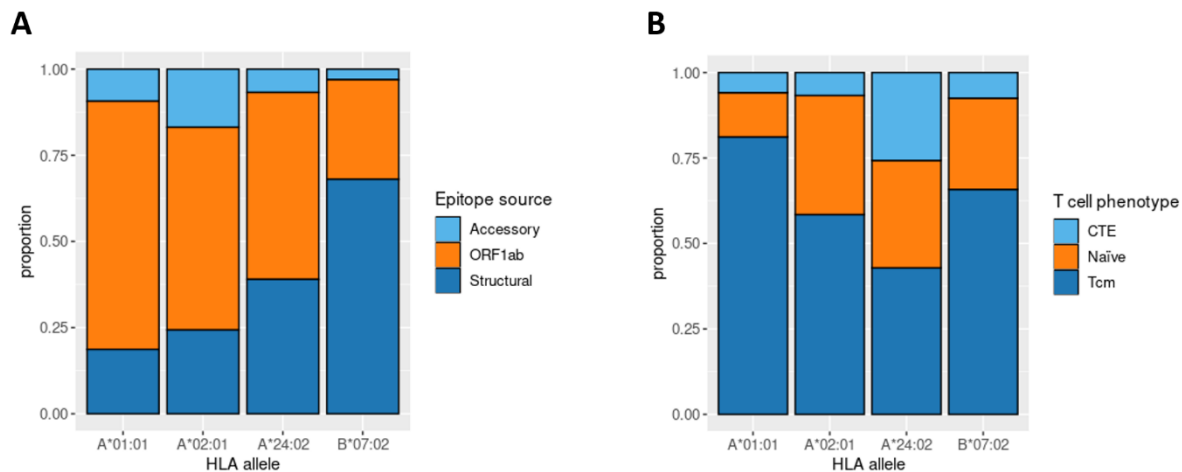


8
9 **Figure 2. The number of virus peptides interacting with the most frequent alleles with an**
10 **affinity of no more than 50 nM.**

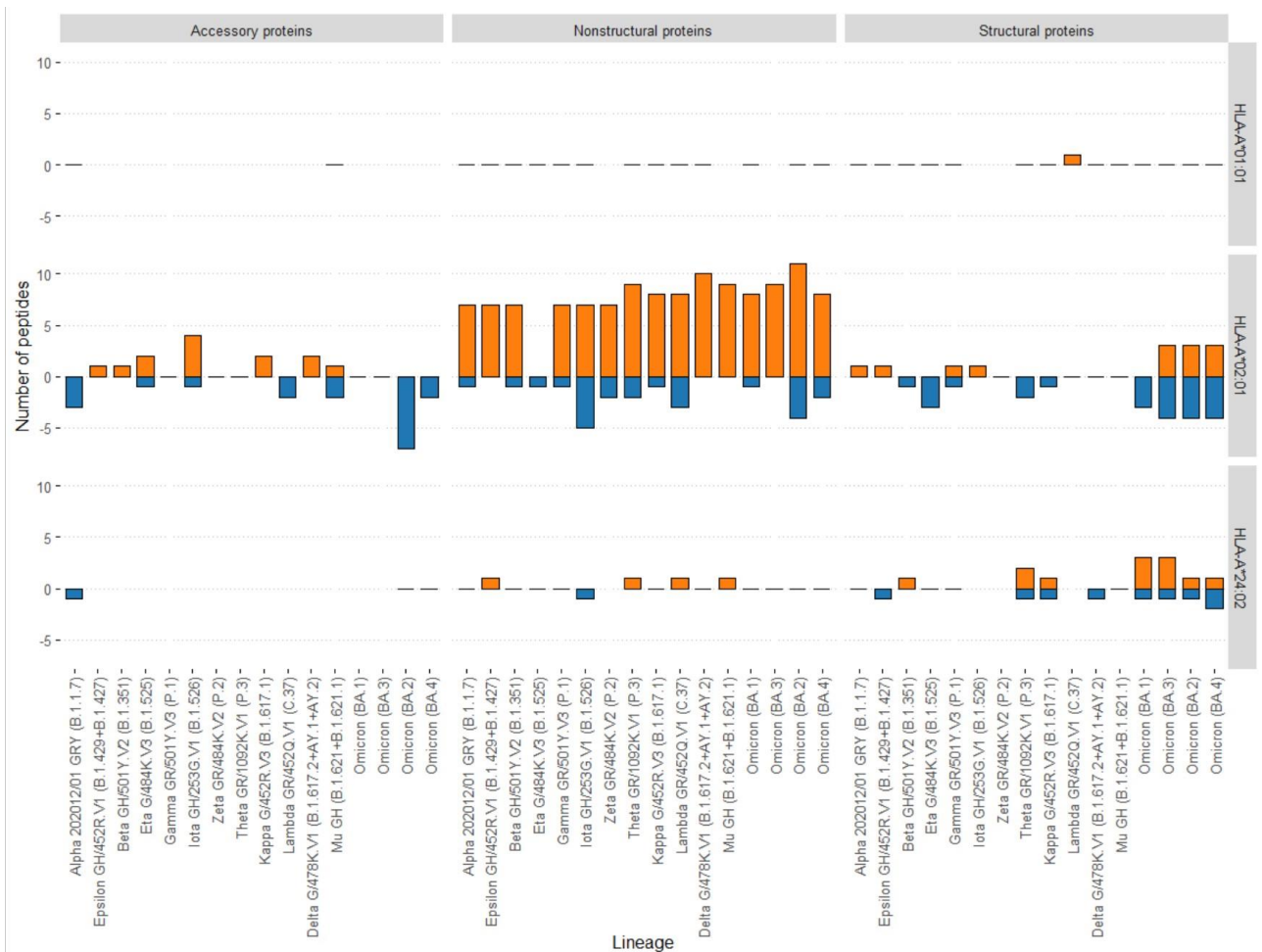
11
12
13



14
15 **Figure 3. Validation of ORF1ab epitopes immunogenicity in a subset of convalescent HLA-**
16 **A*01:01 and HLA-A*02:01 carriers. (A) Distribution of days between symptoms onset and**
17 **blood sampling in the comparison groups. (B) True positive rates for the ORF1ab epitope set**
18 **in the comparison groups.**



19
20 **Figure 4. Phenotype analysis of CD8+ T-lymphocytes of convalescent patients.** (A) The
21 distribution of SARS-CoV-2 derived immunogenic epitopes according to their genomic origin.
22 Epitopes associated with the HLA-A*01:01 allele tend to originate mainly from the
23 conservative ORF1ab region, suggesting a prevalence of memory T-cells among the
24 responding T-cells during the second encounter with SARS-CoV-2. (B) The ratio of responding
25 T-cell phenotypes to the comprehensive set of SARS-CoV-2 derived epitopes. Tcm stands for
26 T central memory subpopulation, and CTE stands for cytotoxic T effector cells. Epitopes
27 associated with the HLA-A*01:01 allele elicit a more robust Tcm response compared with
28 other alleles (pairwise Fisher exact test values: 5.423e-05 for A*01:01 against A*02:02
29 comparison, 0.0178 for A*01:01 against B*07:02 comparison, 6.196e-05 for A*01:01 against
30 A*24:02 comparison).
31

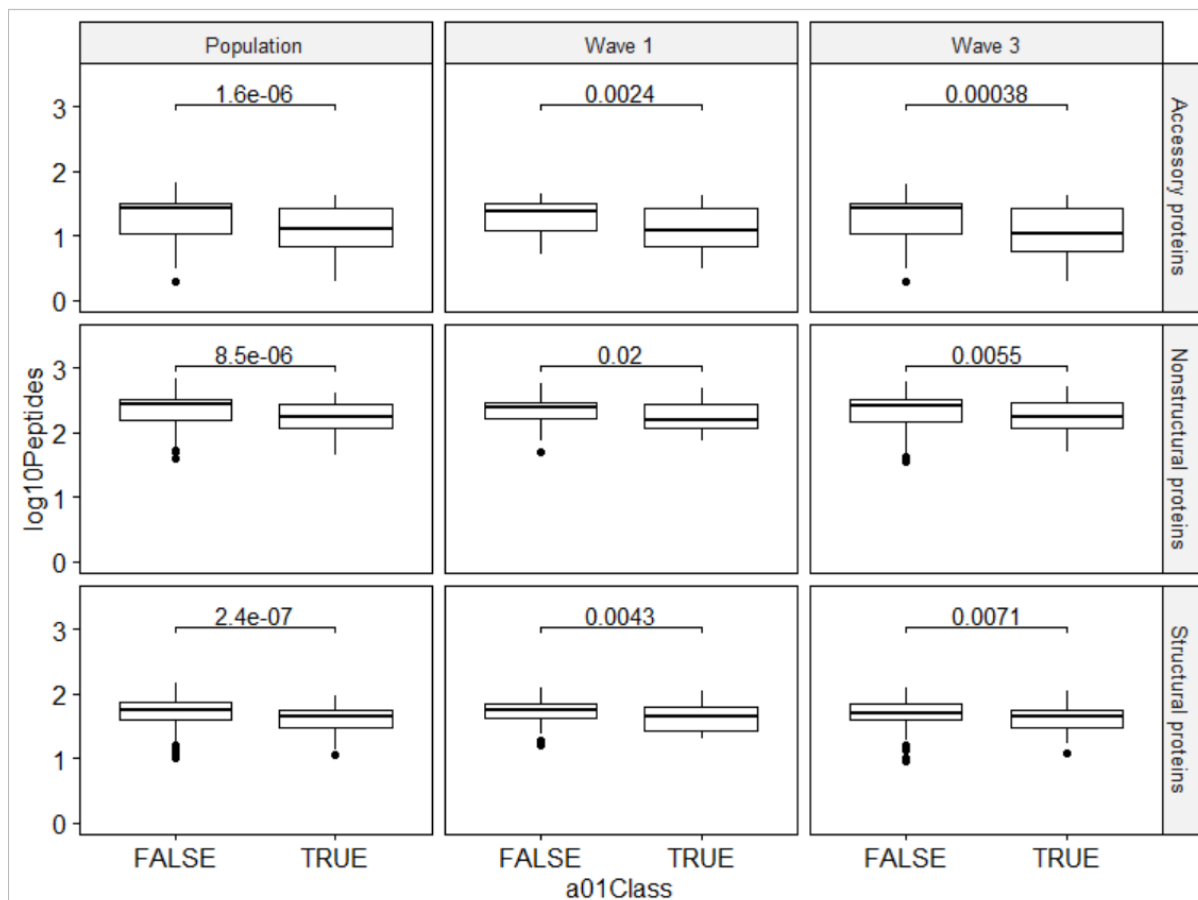


32
33
34
35
36

Figure 5. Effect of mutations in the VOC on the number of tight binders for alleles HLA-A*01:01, HLA-A*02:01, HLA-A*24:02. The orange color bars show the number of peptides that increased the affinity to 50 nM and less; the blue color bars indicate the number of peptides with a decreased affinity to more than 50 nM.

37 Supplementary figures

38



39

40 **Figure S1. The number of unique viral peptides interacting with the sets of HLA molecules**
41 **corresponding to the genotypes (affinity of no more than 50 nM).**

42